ELSEVIER

Thin Solid Films 284–285 (1996) 392–395

thin solid films

Ordering processes at the decanethiol/Au(111) interface

Ornella Cavalleri *, Andreas Hirstein, Jean-Pierre Bucher, Klaus Kern

Institut de Physique Expérimentale, EPF Lausanne, CH-1015 Lausanne, Switzerland

Abstract

Using variable temperature scanning tunnelling microscopy (STM), we studied the ordering processes on thiol-covered Au(111) surfaces at both the mesoscopic and microscopic scale. Because of the chemical erosion accompanying the self-assembly process, thiol-covered gold surfaces present small depressions, a few nanometres in size and one gold layer in depth. These defects can be healed by heating the monolayer up to 350–370 K. By performing isothermal STM measurements at elevated temperature (320–360 K), we followed the growth kinetics of the holes. The vacancy islands are found to coarsen by an Ostwald ripening mechanism. The molecular ordering of the thiol monolayers was also studied. The coexistence of several stable molecular conformations at room temperature was revealed. The well-ordered molecular domains extend over 100–200 Å. The dominant domain configurations contain two superstructures with four molecules per unit cell. The origin of the STM image contrast is discussed.

Keywords: Molecular order; Ostwald ripening; Scanning tunnelling microscopy (STM); Self-assembled monolayers

1. Introduction

In recent years, a large amount of work on the preparation and characterization of self-assembled monolayers has been performed; in particular, alkanethiol monolayers on gold have been the object of extensive investigations performed by different characterization techniques, using electrons, X-rays, thermal helium diffraction, IR spectroscopy and scanning probe microscopy [1]. Most of the interest in these systems arises from the possible production of highly ordered, strongly bound monolayers which not only represent a good model system for molecular interaction studies, but also find technological applications for the control and modification of surface properties, such as adhesion, lubrication, wetting and corrosion inhibition. This explains the importance of obtaining well-ordered, defect-free monolayers. Recently, scanning probe microscopy studies of thiol-covered gold surfaces have revealed the presence of small depressions a few nanometres in size and one gold layer in depth. These depressions have been proven to be vacancy islands in the topmost layer of the gold substrate [2,3], caused by the chemical erosion of gold, probably in the form of a thiol–gold complex, which accompanies the self-assembly process.

In this paper, we report an annealing study of the decanethiol–Au(111) interface; the morphology was followed in situ by variable temperature scanning tunnelling microscopy (STM). The higher mobility at the thiol–gold interface induced by the temperature increase (up to 340–370 K) gives rise to an ordering process, at both the mesoscopic and microscopic scale, which finally results in the healing of the vacancy defects [3,4] and leaves perfectly flat, well-ordered alkanethiolate surfaces. The healing proceeds via vacancy island coarsening (early stage), followed by coalescence (later stage), which, together with annihilation at steps, allows the complete healing of the defects. During vacancy island coarsening, the average island radius is found to increase with time according to the power law $r \propto t^n$, where $n = 1/2$ and t is the observation time whose origin is chosen to correspond to the temperature rise. This power law scaling is consistent with an Ostwald ripening mechanism limited by the detachment rate of vacancies from the hole edges.

The monolayer order was also investigated at the molecular level. The analysis shows the presence of two dominating molecular superstructures with four molecules per unit cell. The average domain size is 100–200 Å at room temperature, but can reach up to 500–600 Å on extensive annealing.

2. Experimental details

Decanethiol ($CH_3(CH_2)_9SH$) monolayers on Au(111) substrates were prepared by the spontaneous adsorption of decanethiol from an ethanol solution. The gold substrates

* Corresponding author. Tel.: +41-21-6933383; fax: +41-21-6933604; e-mail: cavalleri@eldp.epfl.ch.

SSDI 0040-6090(95)08349-9

were prepared by vacuum deposition of a 1000 Å thick gold film on a mica sheet heated at 550 K during deposition, followed by flame annealing in a butane–oxygen flame and quenching in ethanol. STM inspections of the gold surface showed the presence of (111) terraces, 100–300 nm in width, separated mostly by monoatomic steps. After a second flame annealing and ethanol quenching, the substrates, while still covered with ethanol droplets, were immersed in a 1 mM decanethiol solution and kept therein for time periods between 15 and 40 h. The as-prepared samples were thoroughly rinsed with ethanol and then dried in a dry nitrogen flow.

STM measurements were performed with a beetle-type scanning tunnelling microscope whose sample holder was coupled to a Peltier element to allow imaging temperatures from 260 to 400 K (see Ref. [5] for details). Because of its thermal self-compensation, this scanning tunnelling microscope is well suited for variable temperature studies. Isothermal high temperature measurements were performed while flushing the scanning tunnelling microscope compartment with dry nitrogen gas.

3. Results and discussion

In Fig. 1, we show an STM series characterizing the early stage of annealing of a decanethiol-covered Au(111) surface. The three images in Fig. 1(a)–(c) were extracted from an isothermal (350 K) time-lapse sequence of images and were recorded 31, 43 and 52 min after the temperature increase

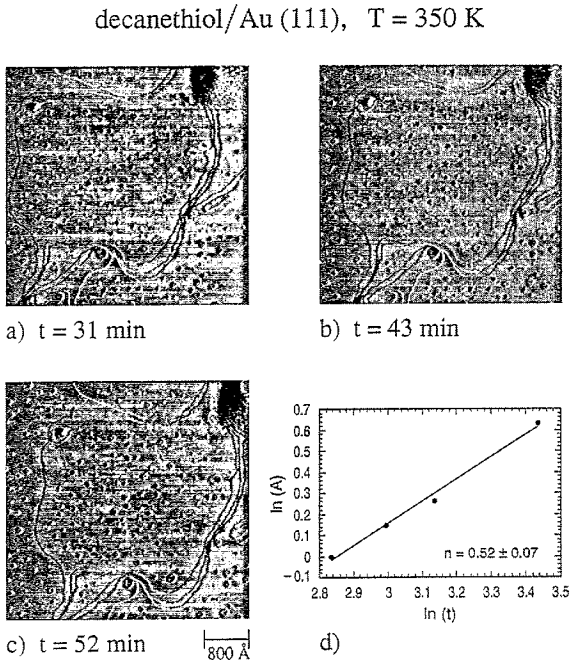

Fig. 1. (a)–(c) Temporal development of the morphology of a decanethiol-covered Au(111) surface during annealing at 350 K. All STM images span 4300 Å×4300 Å. (d) Temporal variation of the average vacancy island size of decanethiol-covered Au(111). Annealing temperature: 350 K. Tunnelling parameters: 1 V, 1 nA.

respectively. The images were acquired in the differential mode, which means that the derivative of the line of constant current is recorded. As can be inferred from the analysis of the three images, the number of holes decreases with time, whereas their average size increases in such a way that, in the absence of annihilation at steps, the total vacancy island area remains constant. The results of a quantitative analysis of the vacancy island growth kinetics are shown in Fig. 1(d). The graph reports, on a logarithmic scale, the average island area (in arbitrary units) vs. the observation time (in minutes) whose origin is chosen to correspond to the temperature increase. The dependence of $\ln(A)$ on $\ln(t)$ is found to be linear with a unitary angular coefficient, which means that the average hole size r scales with time according to $r \propto t^n$, with $n = 0.52 \pm 0.07$.

The observed kinetics of vacancy island growth can be interpreted within the framework of the Ostwald ripening theory as a three-step process involving intralayer mass transport only: (1) desorption of monovacancies from hole edges with high curvature; (2) two-dimensional (2D) diffusion of the monovacancies; (3) re-absorption at hole edges with small curvature. Depending on which of the two processes, namely monovacancy adsorption/desorption at the hole edge or 2D monovacancy diffusion, is the slower, the power in the scaling law $r \propto t^n$ is expected to change from $n = 1/2$ in the former case to $n = 1/3$ in the latter [6]. The measured value of $n \approx 1/2$ indicates that the rate-limiting step for mass transport at the decanethiol–Au(111) interface is the adsorption/desorption rate of monovacancies at the hole edges. The same scenario has also been found for hexanethiol–Au and octadecanethiol–Au interfaces [7]; in both cases, a kinetic exponent of $n \approx 1/2$ has been measured. Although the kinetic growth law of the vacancy mass flow is independent of the thiol chain length, the actual mass flow rate (at a given temperature) has been found to be chain length dependent. For short-chain thiolate monolayers, the healing has been observed to be substantially faster than for long-chain monolayers. This behaviour is not surprising because the emission and diffusion of monovacancies require local rearrangements of thiol molecules which involve interchain bond breaking and making. Thus a larger interchain interaction (i.e. long chains) is expected to slow down the healing process.

Tunnelling microscopy not only provides valuable information on ordering phenomena on the mesoscopic scale, but also gives direct access to molecular ordering. This is demonstrated in Fig. 2(a), which shows a high resolution image of a decanethiol monolayer on Au(111). Prior to imaging (300 K), the sample was annealed for 30 min at 350 K. A nice patchwork of molecular domains is observed with average domain sizes of the order of 100–200 Å. Individual molecular domains are separated by domain boundaries (imaged as depressions) which mainly run along the high symmetry directions of the trigonal substrate. Two domain structures, denoted A and B, each containing four molecules per unit cell, occupy the majority of the surface. In the pin-

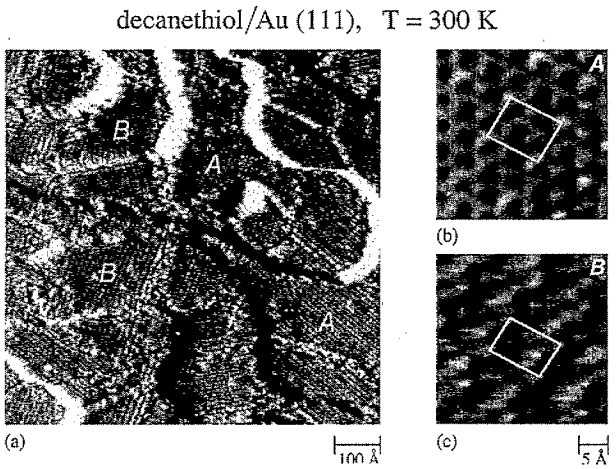

Fig. 2. (a) High resolution image of a decanethiol-covered Au(111) surface showing the dominance of two different types of molecular domain, denoted A and B (see text). The image spans 810 Å×810 Å. (b), (c) Molecular resolution images (29 Å×29 Å) of domain A (pinwheel structure) and domain B (zig-zag structure) respectively. Tunnelling parameters: 1.4 V, 0.8 nA.

wheel structure of domain A (Fig. 2(b)), three of the four molecules per unit cell are symmetry equivalent, whereas in the zig-zag structure of domain B (Fig. 2(c)), two molecules in the unit cell have the same symmetry. The dominance of these molecular domain structures has also been observed in recent STM studies on hexanethiol [8], octanethiol [9] and dodecanethiol [10] monolayers on Au(111). In these studies, the molecular domain ordering was associated with the twist pattern of the alkane chains, similar to that observed in bulk alkane crystals. In order to minimize the mechanical contact between the tip and the molecules, which may influence the orientational order, Anselmetti et al. [10] performed their experiments at a very high tunnelling resistance of several teraohms. This led to the conclusion that tip penetration into the monolayer was avoided and that the tunnelling contrast was mainly due to the outer part of the thiol molecules.

There are several problems with this interpretation. Firstly, the result is not in accord with the loss of ordering of the molecular chains seen in IR spectroscopy and He scattering experiments at 220 K and 100 K respectively [12,11]. Due to its thermal energy (14 meV in Ref. [11]), the probing He beam in the experiment of Camillone et al. [11] does not penetrate the thiol monolayer. He diffraction is thus exclusively sensitive to the ordering of the outermost part of the molecular layer, i.e. the methyl tail groups. According to the experiments in Ref. [11], the ordering of the tail groups disappears at 100 K for an octadecanethiol monolayer. IR spectroscopy, on the other hand, probes the ordering of the entire alkyl chain. With this technique, the orientational ordering is found to persist up to 220 K in the case of a docosanethiol monolayer. In the STM experiments, we can detect supermolecular ordering up to temperatures as high as 340 K. As it is generally accepted that disordering of the alkyl chains propagates from the external to the internal interface with increasing temperature, it is natural to conclude that the sensitivity of tunnelling microscopy must be associated with the molecular structure at the sulphur–gold interface. This interpretation is supported by theoretical calculations which show that the electronic density of states (DOS) near the Fermi level of the sulphur–metal bond is much higher than the respective value of the alkyl chain and should therefore provide the major contribution to the tunnelling current [13]. Further support for this interpretation comes from the fact that supermolecular ordering was imaged in our measurements with conventional tunnelling parameters at potentials of about 1 V and currents of about 1 nA, i.e. an impedance of the order of 1 GΩ, which would probably level out small corrugations of the monolayer by mechanical contact with the tip.

These arguments lead us to exclude the molecular chain origin of these patterns and to conclude that the contrast in the STM images is related to different Au–S–C bonding configurations at the interface. This is in agreement with recent experimental observations which have clearly proven the existence of two different "sulphur species" at the thiol–gold interface [14–16]. The interpretation is further supported by recent ab initio calculations revealing two chemisorption geometries very close in energy: sulphur sp hybridization with an Au–S–C bond angle of approximately 104° and sulphur sp^3 hybridization with a bond angle of approximately 180° [17].

The molecular domains and domain boundaries are not static in nature. At elevated temperatures, the domain walls are mobile, which can be used to increase the average domain size substantially. An example of domain annealing is reported in Fig. 3, which shows two STM images of a decanethiol-covered Au(111) surface recorded at 360 K. The image in Fig. 3(b) was recorded 20 min after that in Fig. 3(a). In both images, we can easily identify the boundaries between different adjacent molecular domains, which are imaged as depressed darker lines. While the average domain size is initially (Fig. 3(a)) of the order of 100–200 Å, it is substantially increased on annealing. In the final state (Fig. 3(b)), the domains reach average sizes as large as 500–600 Å.

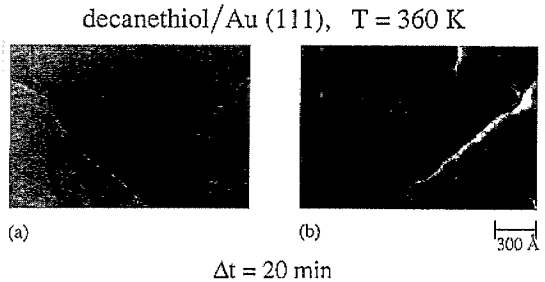

Fig. 3. Mobility of domain boundaries of a decanethiol-covered Au(111) surface at 360 K. STM images span 1750 Å×1150 Å; (b) was recorded 20 min after (a). Tunnelling parameters: 1 V, 0.1 nA. The image in (a) was recorded in the absolute mode, which means that the constant current line is recorded, whereas the image in (b) was recorded in the differential mode.

References

[1] L.H. Dubois and R.G. Nuzzo, *Annu. Rev. Phys. Chem., 43* (1992) 437, and references cited therein.

[2] J.A.M. Sondag-Huethorst, C. Schönenberger and L.G.K. Fokkink, *J. Phys. Chem., 98* (1994) 6826.

[3] J.P. Bucher, L. Santesson and K. Kern, *Langmuir, 10* (1994) 979.

[4] R.L. McCarley, R.J. Dunaway and R.J. Willicut, *Langmuir, 9* (1993) 2775.

[5] J.P. Bucher, H. Röder and K. Kern, *Surf. Sci., 289* (1993) 370.

[6] M. Zinke-Allmang, L.C. Feldman and M.H. Grabow, *Surf. Sci. Rep., 16* (1992) 377.

[7] O. Cavalleri, A. Hirstein and K. Kern, *Surf. Sci.*, in press.

[8] J.P. Bucher, L. Santesson and K. Kern, *Appl. Phys. A, 59* (1994) 135.

[9] G.E. Poirier and M.J. Tarlov, *Langmuir, 10* (1994) 2853.

[10] D. Anselmetti, A. Baratoff, H.J. Güntherodt, E. Delamarche, B. Michel, Ch. Gerber, H. Kang, H. Wolf and H. Ringsdorf, *Europhys. Lett., 27* (1994) 365.

[11] N. Camillone, Ch.E.D. Chidsey, C. Liu and G. Scoles, *J. Chem. Phys., 98* (1993) 3503.

[12] R.G. Nuzzo, E.M. Korenic and L.H. Dubois, *J. Chem. Phys., 93* (1990) 767.

[13] F. Reuse and J.P. Bucher, unpublished results, 1990.

[14] Ch. Zubrägel, C. Deuper, F. Schmeider, M. Neumann, M. Grunze, A. Schertel and Ch. Wöll, *Chem. Phys. Lett., 238* (1995) 308.

[15] M.S. Yeganeh, S.M. Dougal, R.S. Polizzotti and P. Rabinowitz, *Phys. Rev. Lett., 74* (1995) 1811.

[16] P. Fenter, A. Eberhardt and P. Eisenberger, *Science, 266* (1994) 1216.

[17] H. Sellers, A. Ulman, Y. Shnidman and J.E. Eilers, *J. Am. Chem. Soc., 115* (1993) 9389.